American Mineralogist, Volume 64, pages 1063–1074, 1979

Calculation of coherent solvi for alkali feldspar, iron-free clinopyroxene, nepheline–kalsilite, and hematite–ilmenite

JAN TULLIS AND RICHARD A. YUND

Department of Geological Sciences, Brown University
Providence, Rhode Island 02912

Abstract

The coexisting compositions of coherently exsolved phases are given by the coherent solvus. Robin's (1974b) method for calculating the coherent solvus has been modified to allow a more accurate treatment of the compositional strains. Variations in the input parameters for the calculations are considered, and provided that the hydrostatic solvus is accurately known and correctly represented by Margules parameters, the lack of knowledge of the unit-cell parameters at the temperature of exsolution is the principal source of uncertainty for most mineral systems.

The coherent solvus has been calculated for four binary systems. For the monoclinic alkali feldspars, one of the calculated coherent solvi agrees reasonably well with the experimentally determined solvus, except for the Ab-rich limb. The lamellar orientation is predicted to be about ($\bar{8}01$). For the iron-free clinopyroxenes, one of the calculated coherent solvi is depressed only a few degrees below the hydrostatic solvus, and the lamellar orientations predicted are 3° from (001) toward *c*, and 7° from (100) toward *a*. The calculation for the nepheline–kalsilite system requires extrapolation of the unit-cell parameters from nepheline-rich compositions, introducing a large uncertainty. The calculations predict a 350°C depression for (100) lamellae, and a greater depression for (001) lamellae. If a critical temperature of 720°C is assumed for the hydrostatic solvus of hematite–ilmenite, the coherent solvus appears to be depressed about 320°C for (001) lamellae.

Introduction

There has been considerable recent interest in the significance of the orientations and compositions of lamellar intergrowths of minerals resulting from exsolution. Some lamellae are non-coherent; that is, there is no lattice continuity across the lamellar interface. For such cases, Bollman and Nissen (1968) developed a model of optimal phase boundaries which allows one to find the orientation of least lattice mismatch between two phases having nearly parallel crystal axes. Presumably the lamellae boundaries will adopt this orientation of least interfacial energy. Robin's (1977) method, using the Mohr circle, is a simpler and more elegant way of obtaining the orientation of least mismatch, and it also provides the angular deviation of any lattice direction between the two lattices. For these non-coherent lamellae, the cell parameters and compositions will be the same as those for the isolated single-crystal materials.

In contrast, some lamellae are coherent; that is, the lattice is continuous across the lamellar interface. An important consequence of this coherency is that both phases are elastically strained. In this case the orientation of the lamellae will be such as to minimize the elastic strain energy; this includes considerations both of lattice mismatch and of elastic anisotropy for the two phases. Willaime and Brown (1974) have made calculations of the orientations of coherent lamellae for alkali feldspars. However, these calculations do not include a consideration of the compositions of the coherent lamellae.

In general, the compositions of coherent exsolution lamellae, defined by the coherent solvus, are not the same as those for strain-free non-coherent lamellae at the same temperature and confining pressure. These differences arise from the elastic strain energy associated with lattice continuity between phases of different compositions. To date, the coherent solvi for minerals have been investigated only for the alkali

0003–004X/79/0910–1063$02.00

feldspars. These studies include experimental determinations (Yund, 1974; Sipling and Yund, 1976) and theoretical calculations (Robin, 1974a,b).

We have started with Robin's (1974b) elegant formulation for calculating the coherent solvus and have made some modifications in how the compositional strains are treated, included new data for the alkali feldspars, and extended the calculations to three additional binary systems. Another purpose was to determine which of the input parameters in the calculations are the most significant by varying the values of these parameters within reasonable limits to determine the effect of each on the position of the calculated coherent solvus. We believe that these results, together with the additional discussion of the basic procedure, will help to demonstrate both the potential and limitation of this approach, given the data available for most binary mineral systems.

Discussion of method

General considerations

Principles of the calculation of a coherent solvus were first discussed by Cahn (1962), and calculations for alkali feldspars were made by Robin (1974b). In order to calculate the position of the coherent solvus, one would like to know: (1) the unit-cell parameters as a function of composition, temperature, and pressure, in order to calculate the elastic strains associated with coherency at the conditions of exsolution; (2) the elastic constants as a function of composition, temperature, and pressure, in order to derive the elastic stresses associated with the coherency strains and to calculate the total elastic strain energy; and (3) the position of the hydrostatic solvus and a suitable expression for the free energy of the solid solution as a function of temperature and pressure. A brief discussion of these input factors is presented in the following sections, with an emphasis on the modifications that we have made in Robin's (1974b) method.

Calculations of the lattice strains

In order to evaluate the elastic strain energy, the lattice strains associated with the coherency must be known. The stress-free compositional strains are those which are required for a lamella of one composition to match up with a lamella of another composition, in the absence of external stresses. These may include longitudinal strains along a lattice direction, and shear strains associated with changes in lattice angles. Robin (1974b) used a linear approximation for the variation of the monoclinic alkali feldspar unit-cell parameters with composition, choosing his line tangent to each cell parameter curve at the composition of the critical point of the hydrostatic solvus. He then defined compositional strain coefficients which, multiplied by the differences in composition of the lamellae, give the compositional strain (of one lamella relative to the other). For monoclinic symmetry these stress-free compositional strain coefficients are $1/a \cdot \partial a/\partial X$, $1/b \cdot \partial b/\partial X$, $1/c \cdot \partial c/\partial X$, and $\partial\beta/\partial X$, where X is the composition in mole fraction.

The simplification of a linear variation of cell parameters with composition can be avoided if one uses the actual curve for the cell parameter as a function of composition, and calculates the slope of the straight line passing through the values for any two assumed compositions on the coherent solvus. This compositional strain coefficient will give the true strain for these compositions. We have adopted this procedure, and by a process of iteration described below, designed to minimize the elastic strain energy, we are able to obtain the actual strain for the coherent lamellae compositions. This represents our first modification of Robin's (1974b) method.

For most solid-solution series, cell parameters are known as a function of composition at room temperature and pressure, but data may be lacking for the higher temperatures and pressures where exsolution actually occurs. The absolute value of a unit-cell parameter is not important, because strain involves only their differences. However, the thermal expansion may not be the same for both ends of a series, or there may be a structural change in one end of a series between room temperature and the temperature of exsolution. Since the compositional strains are the most important part of the elastic strain energy, this lack of data on cell parameters can be critical, as will be shown by some of the examples we discuss.

Calculation of the principal strains

The stress-free compositional strains for the three lattice directions cannot be used directly to calculate the elastic strain energy. Instead one must derive from them the principal strains (the orthogonal directions of greatest, intermediate, and least compositional strain within the crystal). The symmetry of the principal strains must conform to crystal symmetry. For monoclinic crystals one of the principal strain axes is parallel to the diad axis, usually b, and the Mohr circle can be conveniently used to determine the orientations of the other two axes, which lie in

the a–c plane (Robin, 1974b, 1977). There are two different cases (Fig. 1). In one case (Fig. 1a), the Mohr circle does not intersect the y axis. This happens when all unit-cell parameters in the lamellae of one composition are larger than the corresponding parameters in the lamellae of the other composition. In this case there is a single direction of minimum strain in the a–c plane. In the other case (Fig. 1b) the Mohr circle does intersect the y axis. This happens when some unit-cell parameters in lamellae of one composition are larger and some are smaller relative to the same parameters in lamellae of the other composition. In this case there are two directions of zero strain in the a–c plane. One can determine the value of the minimum strain, as well as the crystallographic orientations of the direction of minimum or zero strain, directly from the Mohr circle (Robin, 1977).

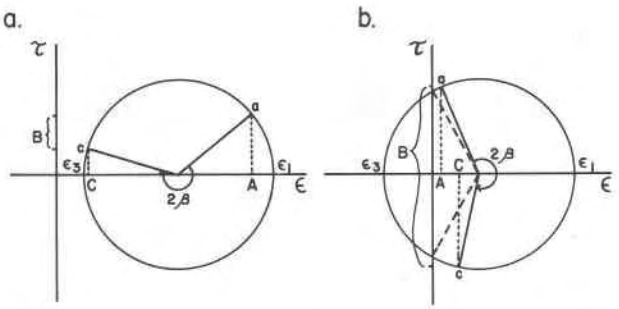

Fig. 1. Examples of Mohr circle construction for determining the stress-free compositional strains in the a–c plane for monoclinic minerals. Shear strains (τ) are plotted on the vertical axis and normal strains (ϵ) on the horizontal axis. The compositional strains parallel to a and c ($1/a \cdot \partial a/\partial X$ and $1/c \cdot \partial c/\partial X$ respectively) are represented by the points A and C. The shear strain in the a–c plane ($\partial\beta/\partial X$) is represented by the interval B. The intercepts of the circle on the ϵ axis define the maximum (ϵ_1 and the minimum (ϵ_3) normal strains. If both a and c increase on going from lamellae of one composition to those of the other composition, then the Mohr circle does not intersect the τ axis and there is one direction of minimum strain, as shown in Fig. 1a. The alkali feldspars are an example of this. If a increases and c decreases (or *vice versa*) on going from lamellae of one composition to those of the other composition, then the Mohr circle does intersect the τ axis and there are two directions of zero normal strain (D), as shown in Fig. 1b. The iron-free clinopyroxenes are an example of this. The crystallographic orientations of these zero or minimum strain directions can be read directly from the diagram.

Elastic anisotropy

Coherency requires that the lattice be continuous between the two coexisting phases, and the lattices of the two phases are therefore elastically stretched or compressed. The elastic anisotropy of the crystal will contribute to determining the interface orientation of minimum elastic strain energy. If the principal compositional strains were all the same, the lamellae would form parallel to the plane containing more compliant directions (those directions for which it takes a lower stress to accomplish the same strain). In fact the anisotropy of the compositional strain is generally more important than the elastic anisotropy, because the compositional strain terms in the expression for the elastic strain energy are squared. For many mineral systems the plane of coherent exsolution will therefore be close to the plane of minimum compositional strain (Willaime and Brown, 1974). The values of the elastic constants will also affect the magnitude of the strain energy and thus the depression of the coherent solvus. Stiffer constants will result in a larger elastic strain energy and a greater depression of the coherent solvus.

For most solid solution series, the elastic constants are not known as a function of composition. In Cahn's (1962) and Robin's (1974b) formulations the strain energy is calculated for the system as a whole, and not separately for the two lamellar compositions, and just one set of elastic constants is used. Ideally one should use the constants for an intermediate composition in the calculations, but using the constants for one end member probably does not introduce serious error. The elastic constants have not been measured as a function of temperature and pressure for most minerals, so we do not know the values appropriate to the actual conditions of exsolution. Again, however, use of room temperature and pressure constants is likely to introduce only small errors in the coherent solvus determination. (See the discussion in Robin, 1974b, p. 1308–1309, and in Willaime and Brown, 1974, p. 326–327.)

Elastic strain energy

From the principal compositional strains and the elastic constants, the elastic stresses and strains associated with coherency on a given plane can be calculated, and these elastic stresses and strains can be used to calculate the elastic strain energy. For minerals of monoclinic or higher symmetry, there will be elastic strains both within the coherency plane and along other directions (including the direction perpendicular to the lamellae), but the only two nonzero principal stresses will be those within the coherency plane. Some of these elastic stresses and strains are known, and some must be solved for. Within the coherency plane, the sum of the elastic strains along each of the two principal directions for the two types of lamellae should be equal to the corresponding

stress-free compositional strains between the two different compositions of lamellae. Knowing these two elastic strains and the (average) elastic constants for the material, we can use Hooke's law ($\tau_i = C_{ij}\ \epsilon_j$ where τ_i are the stress components, ϵ_j the strain components, and C_{ij} the elastic stiffnesses; see Nye, 1957) to write expressions relating the elastic stresses and strains. The two unknown principal stresses in the coherency plane, and the unknown principal strain in the direction normal to the coherency plane, can then be solved for.

Once we know the elastic stresses and strains, we can calculate the elastic strain energy E, which is defined as:

$$E_{ij} = \tfrac{1}{2}\ \tau_i\ \epsilon_j \tag{1}$$

For minerals of monoclinic or higher symmetry there are only two non-zero stresses, and this expression simplifies to:

$$E = \tfrac{1}{2}\ (\epsilon_2\ \tau_2 + \epsilon_3\ \tau_3) \tag{2}$$

where τ_2, τ_3, ϵ_3 are the principal elastic stresses and strains, respectively, within the coherency plane.

Robin (1974b) used stress and strain coefficients instead of stresses and strains, and included the molar volume, in order to write the elastic strain energy in terms of a molar strain energy coefficient k, which yields the strain energy when multiplied by the difference in composition between the lamellae and the bulk:

$$E = k\ (X - X_0)^2 \tag{3}$$

where X is the composition of the lamella and X_0 is the bulk composition, and k has units of cal/mole. We have used this same expression, with the exception that our strains are exact rather than a linear approximation. In addition, we have taken $(X - X_0)$ to be half the compositional difference between the lamellae; thus we assume a slightly different bulk composition for each temperature, if the hydrostatic solvus is asymmetrical. The coherent solvus varies slightly for different bulk compositions (Cahn, 1962), but this should introduce only a slight error into our calculations. We have preliminary experimental data on the position of the coherent solvus for alkali feldspars as a function of bulk composition, indicating that for bulk compositions of Or_{28} and Or_{48}, the position of the coherent solvus varies only a few mole percent at 500° and 530°C.

Coherent solvus

In order to calculate the coherent solvus compositions, Robin (1974b) derived a new function (ϕ), which is equal to the molar Gibbs energy ($\overline{G}$) plus the strain energy term:

$$\phi = \overline{G} + k\ (X - X_0)^2 \tag{4}$$

He then shows that a Margules expansion of ϕ is formally identical to Thompson's (1967) equation (81) for $\overline{G}$, except that W_1 and W_2 in Thompson's equations are replaced by $(W_1 - k)$ and $(W_2 - k)$. W_1 and W_2 are the Margules parameters for $\overline{G}$ and are linearly dependent on temperature and pressure. Thus Robin's equations (E2a) and (E2b) can be used to solve for the coherent solvus compositions which satisfy the expressions for W_1 and W_2, given some value of k. The greater the magnitude of the strain energy coefficient k, the greater the depression of the coherent solvus. Robin (1974b) assumed a linear variation of lattice parameters and no variation of k with temperature, and hence he calculated a single value for k.

We have modified Robin's procedure in order to determine both the orientation and the magnitude of the minimum elastic strain energy coefficient k at each temperature rather than assuming a single value at all temperatures. This procedure represents our second principal modification to his method. Our procedure requires many iterative calculations, so we have incorporated the steps into a computer program. We first *assume* compositions for the coherent solvus at a given temperature, and calculate the resulting lamellar orientation (*i.e.,* that of minimum elastic strain energy) and the elastic strain energy coefficient k. We then use this value for k to resolve Robin's equations (E2a) and (E2b) numerically. If the compositions which satisfy these equations are different from the assumed compositions by more than 0.01 mole percent, the calculation is repeated using the new values of the assumed compositions. Each time new values for the compositional strain coefficients are redetermined from the equations for the cell parameters as a function of composition, a new orientation of the lamellae is calculated, and the elastic strain energy for this orientation is determined. Details and slight differences in the procedure for each of the binary systems are given below.

Obviously one uncertainty in calculating a coherent solvus is the accuracy with which the hydrostatic solvus is known. However, even if the hydrostatic solvus is known exactly, there is still a question as to how well the Margules parameters describe the Gibbs energy for the solid solution. The accuracy of this representation is not well known, and may be an important error in the determination of the coherent solvus for some systems.

Applications

Alkali feldspars

The results for the monoclinic alkali feldspars illustrate many of the practical problems and uncertainties in calculating a coherent solvus. We have tested the effect of variations in the hydrostatic solvus, the cell parameters as a function of composition and temperature, and the elastic constants. We have compared these various calculated solvi with that calculated by Robin (1974b) and with that experimentally determined by Sipling and Yund (1976).

Considerable experimental work has been devoted to determining the position of the hydrostatic solvus, and these studies are discussed and evaluated by Parsons (1978). The earlier data were evaluated by Thompson and Waldbaum (1969), and their estimate for the solvus (TW solvus) was used by Robin (1974b) for his calculations. We have also used the TW solvus for one set of calculations, but we used the 1 bar rather than the 1 kbar solvus. For the other set of calculations we used the results of a study by Smith and Parsons (1974) (SP solvus), which differs from the TW solvus principally on the Or-rich limb as shown by curves a on Figures 2 and 3 respectively. The relations for W_1 and W_2 were calculated from Smith and Parson's (1974) experimental data for run times longer than 2300 hours and for both homogeneous and mixed gel starting materials (curve "C" on their Figs. 5 and 6). We calculated the solvus for 1 bar using their value of 16°C/kbar for dT_{crit}/dP, and the expressions for W_1 and W_2 are given in the Appendix.

We have used two sets of relations for the cell parameters as a function of composition. The first set is Orville's (1967) room-temperature cell parameters for the sanidine–high albite series. Although accurately determined, these are not necessarily the best values for our purpose. Our calculations assume monoclinic symmetry for both phases, which is probably correct at the temperature of exsolution for most bulk compositions (Sipling and Yund, 1976). However, Orville's compositions between Or_0 and Or_{35} are triclinic at room temperature, because of the nonquenchable monoclinic–triclinic transformation in Ab-rich compositions (Kroll and Bambauer, 1971). Thus the cell parameters in this compositional interval are not strictly applicable for our calculations at higher temperatures where the Ab-rich compositions are monoclinic. Robin (1974b) has also used Orville's (1967) cell parameters for his calculations, although he has assumed a linear relation, by taking the slopes of tangents at a bulk composition of Or_{33}.

Our second set of cell parameters is estimated for 500°C from thermal expansion data. We have used the data for Or_{100}, Or_{40}, and Or_{20} from Henderson and Ellis (1976), and the data for Or_0 from Grundy and Brown (1969). The cell parameter curves as a function of composition are essentially parallel at all temperatures, and we have arbitrarily chosen to use the parameters for 500°C for all solvus temperatures. These second-order polynomial relations are given in the Appendix.

Table 1 illustrates how these two sets of cell parameters affect the calculations. The first four columns list the stress-free compositional strains for coexisting compositions of Or_{14} and Or_{61}, near the critical temperature of the coherent solvus, for the two sets of cell parameters. The high-temperature parameters give significantly lower strains. Table 1 also shows that the direction of minimum compositional strain varies somewhat with the coexisting compositions and with the cell parameters. (See Willaime and Brown, 1974, Table 3, for similar calculations.) The elastic constants for feldspar are poorly known (Willaime and Brown, 1974; Robin, 1974b; Tullis, 1975), but the elastic anisotropy does not strongly affect the lamellar orientation; the plane of minimum elastic strain energy is essentially the same as the plane of minimum compositional strain. Table 1 gives values of the elastic strain energy coefficient calculated using Robin's (1974b) stiffer set of elastic constants. The last two columns show how this coefficient varies with the cell parameters and with the coexisting compositions. These values should be compared with the single value that Robin (1974b) obtained (704.6 cal/mole), using the linear approximation of the room-temperature cell parameters.

The results for some of our calculations of the coherent solvi are shown in Figures 2 (TW solvus) and 3 (SP solvus). The coherent solvus shown on both figures as curve b is the one determined experimentally by Sipling and Yund (1976). There is an uncertainty in the location of their solvus, especially the Ab-rich limb, of probably a few mole percent, because of experimental error and the fact that the compositions determined from X-ray data must be corrected for elastic strain using the method of Tullis (1975). However, this experimentally determined solvus is a valuable reference for the calculated curves, in part because its determination is independent of the position of the hydrostatic solvus.

Robin (1974b) calculated the coherent solvus for

Table 1. Calculated parameters for alkali feldspars

	Stress-free compositional strains (%)*				Direction of minimum compositional strain (degrees from c toward a)**		Strain energy coefficient k (cal/mole)***	
	a	b	c	β	520°C	300°C	520°C	300°C
25°C cell parameters	2.67	0.75	0.52	0.29	7.7	8.6	819	614
500°C cell parameters	2.98	0.51	0.48	0.19	9.3	9.7	460	347

*For co-existing compositions of Or_{14} and Or_{61}.

**The plane of minimum compositional strain includes this direction and the b axis.

***Strain energy calculated using Robin's (1974b) stiffer set of elastic constants.

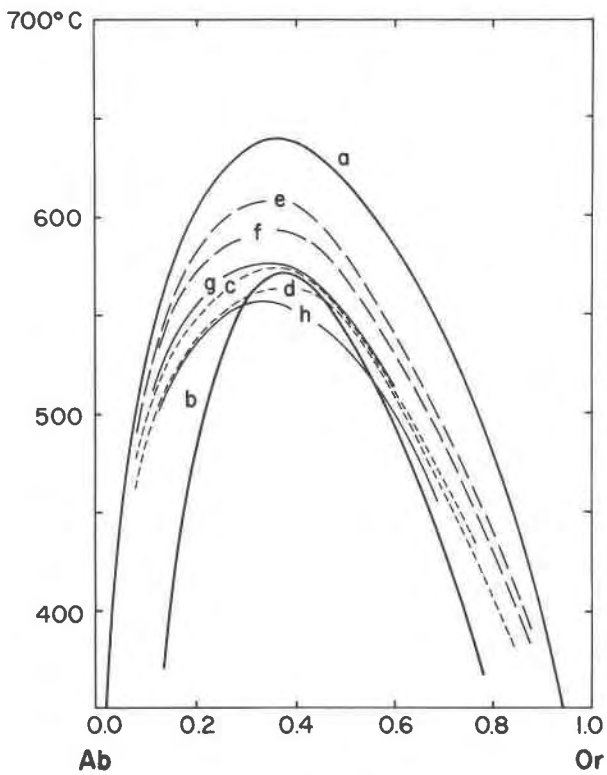

Fig. 2. Temperature–composition diagram for alkali feldspar, showing calculations based on the hydrostatic solvus of Thompson and Waldbaum (1969), which is shown for 1 bar by curve a. Curve b is the coherent solvus experimentally determined by Sipling and Yund (1976). Curves g and h are the coherent solvi calculated by Robin (1974b) for the less stiff (g) and stiffer (h) set of elastic constants. Curves c and d are the coherent solvi we have calculated using the same room-temperature cell parameters and the same elastic constants, but calculating the compositional strains more accurately. Curves e and f are the coherent solvi we have calculated using the estimated high-temperature cell parameters and the same elastic constants.

the two sets of elastic constants using the 1 kbar TW solvus. We have recalculated his curves, using his exact method except with the 1 bar solvus data. These are shown by curves g and h on Figure 2; the stiffer elastic constants result in a coherent solvus which is more depressed. Our results for the room-temperature cell parameters, using the same elastic constants but calculating the compositional strain more accurately and separately at each temperature, are shown by curves c and d on Figures 2 and 3. Our results for the 500°C cell parameters, again for the two sets of elastic constants, are shown by curves e and f on Figures 2 and 3. The 500°C cell parameters result in lower compositional strains, and thus coherent solvi which are less depressed.

For calculations based on the TW solvus (Fig. 2), the difference between Robin's (1974b) calculated coherent solvi and ours is small. Our curves for the room-temperature cell parameters are only slightly closer to the experimental coherent solvus, despite our more accurate calculation of the compositional strains at each temperature. This suggests that improvements in the calculated coherent solvus must involve changes in the other input parameters.

For the TW solvus, it is interesting that the 500°C cell parameters provide a much worse fit to the experimental solvus. In addition, for the room-temperature cell parameters, the less stiff elastic constants provide a better fit to the experimental solvus, for both Robin's calculations and ours. It would seem more reasonable for the high-temperature cell parameters and the stiffer elastic constants to provide a better fit, and this is seen to be the case for our calculations based on the SP solvus (Fig. 3, curve f). This

calculated curve provides a good fit for the depression of the crest and the position of the Or-rich limb, compared to the experimental coherent solvus (curve b). However, the Ab-rich limb is too wide on this (as well as all other) calculated coherent solvus. Changes in the elastic constants cannot improve the fit on this limb. One possible explanation is the uncertainty in the Ab-rich cell parameters, as already noted; this affects both the corrections applied to the experimental compositions on this limb, as well as the calculations of the coherent solvus. In addition to the uncertainty in the hydrostatic solvus compositions, there is a question as to how accurately the Margules parameters represent the Gibbs energy as a function of composition.

Another factor, probably less significant, is related to a fundamental aspect of Robin's (1974b) and Cahn's (1962) formulation. The elastic strain energy, and hence the coexisting compositions, are independent of the bulk composition only if the elastic constants and the compositional strain coefficients do not vary with composition. As the volume fraction of one phase decreases it will be strained more relative to the dominant phase, and this will result in an overall increase in the total elastic strain energy if the phases have different elastic constants. A completely new formulation would be necessary to take this into account, and given the present uncertainty in the data it is not worthwhile to attempt this.

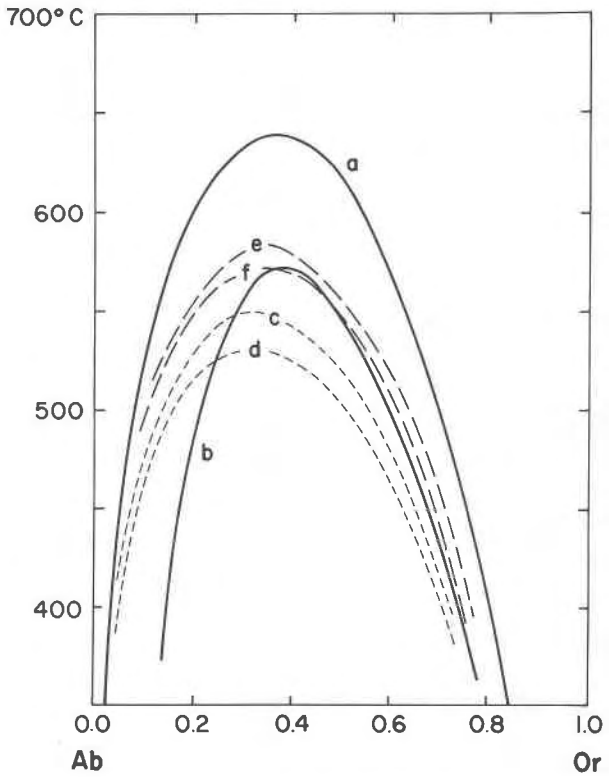

Fig. 3. Temperature–composition diagram for alkali feldspars, showing calculations based on the hydrostatic solvus of Smith and Parsons (1974), which is shown for 1 bar by curve a. Curve b is the coherent solvus experimentally determined by Sipling and Yund (1976). Curves c and d are the coherent solvi we have calculated using the room-temperature cell parameters; c represents the less stiff elastic constants, and d the stiffer set. Curves e and f are the coherent solvi we have calculated using the estimated high-temperature cell parameters and the same elastic constants.

Iron-free clinopyroxenes

The hydrostatic solvus for iron-free pigeonite is not well known. We have used the one-bar solvus from Kushiro's (1972) Figure 2. The diopside-rich side of the solvus is largely from Boyd and Schairer (1964). We assume that the iron-free pigeonite in Kushiro's diagram has the diopside structure ($C2/c$) at high temperature. We have extrapolated the solvus metastably above the incongruent melting temperature (~1388°C) and below the breakdown to protoenstatite and diopside (1200–1300°C) by using the "r–s" method of Thompson and Waldbaum (1969). This is shown as curve a on Figure 4. The relations for W_1 and W_2 are given in the Appendix.

Cell parameters for clinopyroxenes as a function of composition at room temperature were reported by Turnock *et al.* (1973). New cell parameters were recently published by Newton *et al.* (1979); their values are in good agreement and would not significantly change our results. The Mg-rich compositions probably do not have the $C2/c$ structure. Smith (1969a) and others have shown that there is a significant difference between the room- and high-temperature cell parameters for these compositions. Thus we have used three sets of cell parameters. One is a third-order polynomial fit to the room-temperature data from Turnock *et al.* (1973). Second is a linear fit to only the diopside-rich compositions, extrapolated into the Mg-rich regions. We believe, however, that a third set is best even though it is based on only two compositions. These are the 1100°C values for $Mg_{1.9}Ca_{0.1}Si_2O_6$ reported by Smith (1969b), and the 1100°C values for diopside calculated from the high-temperature thermal expansion data of Cameron *et al.* (1973). We will refer to these as the third-order polynomial, the linear, and the high-temperature data sets, respectively. The equations describing the cell parameters for these three data sets are given in the Appendix.

In contrast to the alkali feldspars, the Mohr circle

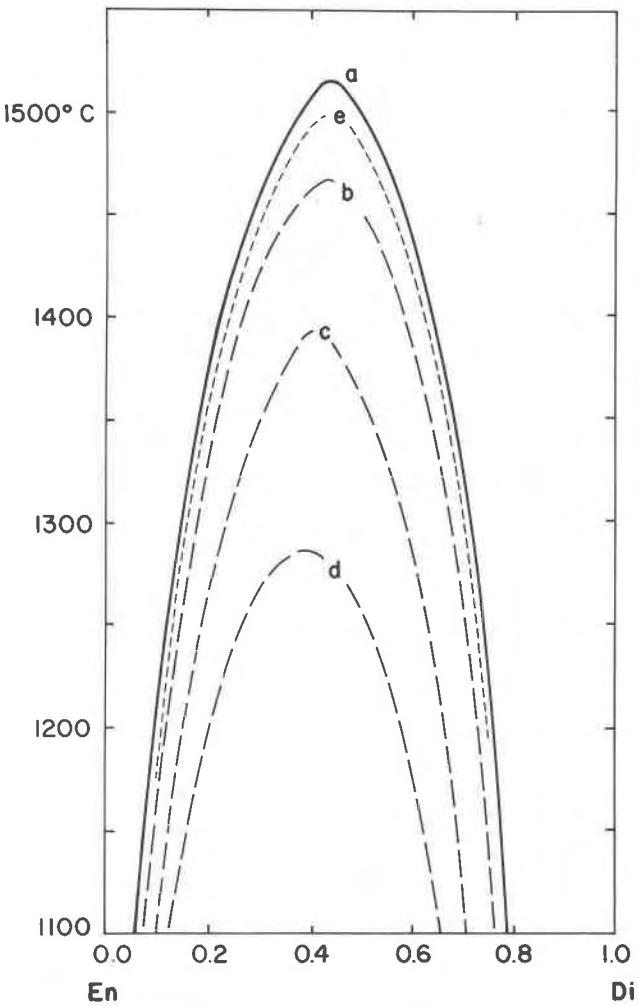

Fig. 4. Temperature–composition diagram for iron-free clinopyroxenes. Curve a is the hydrostatic solvus, taken from Kushiro (1972) and Boyd and Schairer (1964), and extrapolated metastably to higher and lower temperatures. Curves b, c, and d are the coherent solvi we have calculated based on the room-temperature cell parameters of Turnock *et al.* (1973); curve b is for the orientations of zero compositional strain, 17° and 48° from *a* away from *c*; curve c is for (001) orientations; and curve d is for (100) orientations. Curve e is the coherent solvus we have calculated based on the linear fit to the room-temperature cell parameters, for the two directions of zero compositional strain, (100) and 7° from *c* toward *a*. The coherent solvus we have calculated based on the high-temperature cell parameters is essentially indistinguishable from the hydrostatic solvus, and so is also represented by curve a.

for the compositional strains for the iron-free clinopyroxenes intersects the *y* axis, as shown in Figure 1a. Thus there are two directions of *zero* longitudinal strain in the *a–c* plane, rather than a single direction of *minimum* strain as was true for the alkali feldspars. In fact the compositional strains in any direction within the *a–c* plane are small, and thus the particular values of the cell parameters are very important for predicting the lamellae orientation. This is shown clearly in Table 2. However, the coherency strain and the depression of the coherent solvus are due primarily to the misfit along *b*. The compositional strains for coexisting compositions of Di_{29} and Di_{58}, for the three sets of cell parameters, are given in Table 2. The high-temperature cell parameters give lower strains and hence a coherent solvus which is less depressed.

We have used the room-temperature elastic constants for diopside (composition not given) measured by Aleksandrov *et al.* (1964), with the correction that C_{15}, C_{25}, C_{35}, and C_{46} are positive (Baker and Carter, 1972). We have also done calculations for the case where each of these stiffnesses is multiplied by 1.1 and by 1.2. In addition we have done calculations using the room-temperature constants for augite measured by Aleksandrov *et al.* (1964). In all cases the planes of minimum elastic strain energy are essentially the same as the planes of zero compositional strain listed in Table 2, and the differences between the various coherent solvi are negligible.

Some of our calculated coherent solvi are shown on Figure 4. For the third-order polynomial data, the coherent solvus for the directions of zero compositional strain (orientations given in Table 2) is shown as curve b. For comparison, we have calculated the coherent solvus for two fixed orientations, (001) (curve c, k is approximately 650 cal/mole) and (100) (curve d, k is 1060 cal/mole). The coherent solvi for these orientations are depressed more than twice as much as that for the zero strain directions, and thus one should not expect to see coherent lamellae with these orientations in slowly cooled rocks. Fletcher and McCallister (1974) calculated the crest of the coherent spinodal, which must be tangent to the crest of the coherent solvus, for (001) orientations for iron-free pyroxenes, using room-temperature cell parameters. They calculated a depression of 110°C, which is in good agreement with our value of 120°C.

For the linear cell parameter data, the coherent solvus for the two orientations of zero stress-free compositional strain is shown by curve e on Figure 4. For the high-temperature cell parameter data, the coherent solvus for the two orientations of zero stress-free compositional strain is only depressed below the hydrostatic solvus by a few degrees, and hence is not shown on Figure 4.

There is no experimentally determined coherent

Table 2. Calculated parameters for iron-free clinopyroxenes

	Stress-free compositional strains (%)*				Directions of zero compositional strain in the a-c plane**		Strain energy coefficient k (cal/mole)***	
	a	b	c	β	1450°C	1100°C	1450°	1100°
25°C cell parameters (polynomial)	0.37	0.38	0.59	0.88	13° from c 21° from a	22° from c 29° from a	189 189	209 209
25°C cell parameters (linear)	0.24	0.24	0.00	0.82	7° from c parallel to c	7° from c parallel to c	70 66	70 66
1100°C cell parameters	0.11	0.12	0.28	1.15	3° from a 7° from c	3° from a 7° from c	20 (16) 20 (16)	20 (16) 20 (16)

*For co-existing compositions of Di_{29} and Di_{58} ($Mg_2Si_2O_6$ and $CaMgSi_2O_6$ end members).

**All directions lie between positive a and c. The planes of zero compositional strain include these directions and the b axis.

***Calculated using the room temperature stiffnesses for diopside; values in parentheses were calculated using the room temperature stiffnesses for augite (Aleksandrov et al., 1964)

solvus for the iron-free clinopyroxenes, so we cannot say which set of cell parameters yields the best coherent solvus. However, McCallister and Yund (1977) have observed coherent lamellae parallel or within a degree or two of (001) in experimentally exsolved iron-free clinopyroxenes. This orientation is close to one of the directions of zero stress-free compositional strain for the high-temperature cell parameter data (see Table 2), and thus we believe this set of calculations is preferred. Further refinements would require more accurate high-temperature cell parameter data as well as better data for the elastic constants. However, no matter what the exact values, the depression of the coherent solvus will be smaller for these pyroxenes than for the alkali feldspars, because they have directions of zero strain in the *a–c* plane. This probably explains why the coherent solvus has not been recognized in phase equilibria studies employing exsolution experiments (*i.e.*, Boyd and Schairer, 1964).

It should not be assumed that the coherent solvus for iron-bearing pyroxenes will have the same depression as that for the iron-free system, because both the cell parameters and elastic constants will be different. Given the uncertainty in the hydrostatic solvus and cell parameters for the iron-bearing pyroxenes, we do not believe that calculations of the coherent solvi would be worthwhile. The orientation of exsolution lamellae in iron-bearing pyroxenes has been discussed by Robin (1977) and Robinson *et al.* (1977).

Nepheline–kalsilite

The equilibrium solvus and cell parameters for nepheline–kalsilite have been recently redetermined by Ferry and Blencoe (1978). However, the crystal structure of $P6_3$ nepheline ($a \approx 10$A) is not the same as $P6_3$ kalsilite ($a \approx 5$A), and hence the critical point (~1240°C at 0.5 kbar) is metastable. Because of this structural difference, we have extrapolated the room-temperature cell parameter data from the nepheline-rich compositions to the kalsilite-rich compositions (see Appendix). This introduces an unknown but potentially large error in the calculations of the coherent solvus for this system.

Within the limitations noted above, there is no direction of stress-free compositional strain, and the strains along *a* and *c* are both about 2 percent. We have calculated coherent solvi for both (100) and (001) lamellar orientations; the crests of the two solvi are at about 750° and 570°C, respectively. These calculations are based on the less stiff of two sets of elastic constants (Ryzhova and Aleksandrov, 1962). Using the stiffer set lowers the coherent solvus only

about 20°C, which is probably much less than the uncertainty originating from the compositional strains.

Although the (001) coherent solvus is calculated to be the more depressed, in nature one observes only basal orientations of lamellae, ranging from 'cryptoperthites' to coarse blebs and lamellae (Sahama, 1960). To our knowledge there are no observations regarding the coherency of these 'cryptoperthite' lamellae. Almost all the kinetic data for exsolution in this system reported by Yund *et al.* (1972) were obtained at 600°C, but they did not determine the orientation of the exsolved phase, or whether it was coherent or not. Nevertheless, exsolution appears to be very rapid in this system at all temperatures above 600°C, and coherent nepheline–kalsilite intergrowths in nature would be unlikely except in the most rapidly cooled volcanic rocks.

Although our calculations suggest that the coherent solvus would be accessible to experimental determination, the relative ease of diffusion of all species in nepheline–kalsilite compared to feldspars and pyroxenes suggests that coherent lamellae (if they ever form) might start to lose coherency even in laboratory experiments. In fact, this might be a suitable silicate system to study how the loss of coherency occurs.

Hematite–ilmenite

Within the constraints set by Lindsley (1973), we have arbitrarily guessed a hydrostatic solvus with a critical temperature of 720°C at 46 mole percent ilmenite. Thus our calculations are useful only for showing the *relative* depression of the coherent solvus. Elastic constants for hematite were measured by Voight (1907), although Birch (1965) believes the values to be somewhat suspect. The expressions for W_1 and W_2 and the cell parameter data are given in the Appendix. The stress-free compositional strain is greater parallel to c than to a; hence the lamellar orientation is expected to be (001). For this orientation, we calculate the crest of the coherent solvus to be depressed by 320°C.

Natural hematite–ilmenite solid solutions have exsolution lamellae parallel to (001) in both metamorphic (Rumble, 1976) and igneous (Haggerty, 1976) rocks. Lally *et al.* (1974) reported that the lamellar interface of a natural sample consisted of an array of dislocations and that the phases were semi-coherent. Further studies are needed of intermediate hematite–ilmenite compositions which appear optically homogeneous, to determine whether they have a coherent lamellar microstructure. The relatively large depression of the coherent solvus indicates that it is probably not accessible to experimental study, because the diffusivities of the Fe and Ti ions would be too low to achieve exsolution in laboratory times at these low temperatures (≤400°C). Thus studies concerned with how this exsolution microstructure forms may be restricted to examination of natural specimens.

Conclusions

A knowledge of the coherent solvus is important for understanding the exsolution behavior of minerals. The three principal factors which enter into a calculation of the coherent solvus are: the average elastic constants for the mineral; the cell parameters as a function of composition; and the position of the hydrostatic solvus and its representation by Margules parameters.

Although the elastic constants for many minerals are only poorly known, an uncertainty of 20 percent in these values changes the depression of the coherent solvus by only about 20°C, as shown for the alkali feldspars and iron-free clinopyroxenes. This suggests that use of room-temperature and -pressure elastic constants for one end member of a solid-solution series, instead of those for an average composition at the temperature and pressure of exsolution, should not introduce serious error.

Uncertainty in the cell parameters as a function of composition at the exsolution temperature is a major source of error, because the compositional strains are the dominant term in the strain energy expression. For example, quite different results are obtained for the iron-free clinopyroxenes depending on whether one uses the room-temperature cell parameters or the estimated high-temperature data. This problem is especially critical when there is a structural discontinuity in the solid-solution series at the temperature where the cell parameters were measured. This is the case for the monoclinic alkali feldspars and for nepheline–kalsilite, and introduces a potentially large but unknown uncertainty in the calculated coherent solvus for these systems.

Clearly any uncertainty in the position of the hydrostatic solvus is critical, and for a system such as hematite–ilmenite in which the hydrostatic solvus is not known, only a relative depression of the coherent solvus can be calculated. Another error, of unknown magnitude, concerns how well the Margules parame-

ters represent the Gibbs energy as a function of composition and temperature. Our modification of Robin's method does not significantly improve the fit to the experimentally determined coherent solvus for the alkali feldspars, using the Thompson–Waldbaum data for the hydrostatic solvus and the room-temperature cell parameters. However, use of the recent Smith-Parsons hydrostatic solvus together with the 500°C cell parameters significantly improves the fit, although the Ab-rich limb is still too wide compared to the experimental coherent solvus. Changes of the cell parameters cannot change the position of one limb of the coherent solvus, and hence this lack of agreement must be due to other causes. The most likely source of error is either the position of the hydrostatic solvus, or the correctness of the Margules parameters for representing the Gibbs function. Another possible explanation is that the experimentally determined position of the Ab-rich limb is incorrect.

Most of the common binary mineral systems are subject to one or more of the above uncertainties. Hence, at present, an accurate evaluation of the coherent solvus for most systems requires experimental verification. However, calculations of the coherent solvus are useful as a guide for experimental studies, or for qualitatively predicting and interpreting exsolution behavior in minerals.

Acknowledgments

We wish to thank T. Tullis for helpful discussions and R. McCallister for comments on the manuscript. We particularly wish to thank P.-Y. Robin for stimulating discussions and a critical review of the manuscript which resulted in many improvements; any mistakes, however, are entirely our own. This work was supported by NSF grant EAR75-21791 to RAY.

References

Aleksandrov, K. S., T. V. Ryzhova and B. P. Belikov (1964) The elastic properties of pyroxenes. *Bull. (Izv.) Acad. Sci. USSR, Kristallogr.* [transl. *Am. Geophys. Union,* 589–591 (1964)].

Baker, D. W. and N. L. Carter (1972) Seismic velocity anisotropy calculated for ultramafic minerals and aggregates. In *Flow and*

Appendix

A. Alkali Feldspars

1. Margules parameters for 1 atmosphere solvus

a. Thompson and Waldbaum (1969)

$W_1 = 6327.0 - 4.632\ T$

$W_2 = 7672.0 - 3.857\ T$

b. Smith and Parsons (1974)

$W_1 = 2004.0 + 0.469\ T$

$W_2 = 7638.6 - 4.023\ T$

2. Cell parameters as a function of composition (in mole percent Or)

a. Room temperature data (Orville, 1967)

$a = 8.15328 + 0.36749\times10^{-2}\ X + 0.2687\times10^{-4}\ X^2 - 0.18688\times10^{-6}\ X$

$b = 12.85722 + 0.40877\times10^{-2}\ X - 0.3156\times10^{-4}\ X^2 + 0.7217\times10^{-7}\ X^3$

$c = 7.1115 + 0.16805\times10^{-2}\ X - 0.15067\times10^{-4}\ X^2 + 0.4937\times10^{-7}\ X^3$

$\beta = 116.47 - 0.31776\times10^{-2}\ X - 1.2503\times10^{-4}\ X^2 + 1.127\times10^{-6}\ X^3$

b. 500°C parameters from thermal expansion data of Henderson and Ellis (1976), and Grundy and Brown (1969).

$a = 8.202 + 5.1587\times10^{-3}\ X - 4.7445\times10^{-6}\ X^2$

$b = 12.901 + 3.088\times10^{-3}\ X - 1.8805\times10^{-5}\ X^2$

$c = 7.129 + 1.3146\times10^{-3}\ X - 8.2804\times10^{-6}\ X^2$

$\beta = 116.32 - 8.0\times10^{-3}\ X + 4.21\times10^{-5}\ X^2$

B. Iron-free Clinopyroxenes

1. Margules parameters for 1 atmosphere solvus, from Kushiro (1972) and Boyd and Schairer (1964)

$W_1 = 1804.7 + 2.619\ T$

$W_2 = 10{,}691.1 - 1.797\ T$

2. Cell parameters as a function of composition (in mole percent Di)

a. Room temperature data (Turnock et al., 1973)

$a = 9.5917 + 0.4411\times10^{-2}\ X - 0.5412\times10^{-4}\ X^2 + 0.2582\times10^{-6}\ X^3$

$b = 8.8111 + 0.2338\times10^{-2}\ X - 0.1727\times10^{-4}\ X^2 + 0.5668\times10^{-7}\ X^3$

$c = 5.1566 + 0.2483\times10^{-2}\ X - 0.1712\times10^{-4}\ X^2 + 0.1362\times10^{-7}\ X^3$

$\beta = 108.16 + 0.3600\times10^{-1}\ X - 0.1295\times10^{-2}\ X^2 + 0.7068\times10^{-5}\ X^3$

b. Room temperature data for diopside (straight line fit to compositions $\geq$ 58.4 mole percent Di)

$a = 9.67 + 0.8\times10^{-3}\ X$

$b = 8.86 + 0.7\times10^{-3}\ X$

$c = 5.25$

$\beta = 109.15 - 0.335\times10^{-1}\ X$

c. 1100°C data from Smith (1969b) and Cameron et al. (1973)

$a = 9.870 - 0.4\times10^{-3}\ X$

$b = 8.952 + 3.7\times10^{-4}\ X$

$c = 5.338 - 5.2\times10^{-4}\ X$

$\beta = 110.4 - 4.3\times10^{-2}\ X$

C. Nepheline-Kalsilite

1. Margules parameters calculated from the 0.5 kbar data of Ferry and Blencoe (1978)

$W_1 = 7462.2 - 2.29\ T$

$W_2 = 3005.0 + 1.77\ T$

2. Cell parameters as a function of mole percent Ks $[Na_3K(AlSiO_4)_4 - K_4(AlSiO_4)_4]$, based on compositions from 3.1–22.9 mole percent Ks (Ferry and Blencoe, 1978)

$a = 10.0023 + .00319\ X$

$c = 8.3877 + .00181\ X$

$a^* = .11544 - 3.65\times10^{-5}\ X$

D. Hematite-Ilmenite

1. Margules parameters for 1 atmosphere solvus, guessed given the constraints of Lindsley (1973)

$W_1 = 970.3 + 2.804\ T$

$W_2 = 755.8 + 3.376\ T$

2. Cell parameters as a function of composition at room temperature, from Lindsley (1965) (in mole percent Ilm)

$a = 5.035 + 0.3606\times10^{-3}\ X + 0.3284\times10^{-5}\ X^2 - 0.1505\times10^{-7}\ X^3$

$a^* = .2289 - 0.3929\times10^{-4}\ X + 0.1786\times10^{-6}\ X^2 - 0.2909\times10^{-19}\ X^3$

$c = 13.741 + 0.2848\times10^{-2}\ X + 0.1229\times10^{-4}\ X^2 - 0.1736\times10^{-6}\ X^3$

Fracture of Rocks, p. 157–166. Am. Geophys. Union Monogr. 16.

Birch, F. (1965) Compressibility; elastic constants. In S. P. Clark, Jr., Ed., *Handbook of Physical Constants,* p. 97–174. Geol. Soc. Am., New York.

Bollman, W. and H. U. Nissen (1968) A study of optimal phase boundaries: the case of exsolved alkali feldspars. *Acta Crystallogr., A24,* 546–557.

Boyd, F. R. and J. F. Schairer (1964) The system $MgSiO_3$–$CaMgSi_2O_6$. *J. Petrol., 5,* 545–560.

Cahn, J. W. (1962) Coherent fluctuations and nucleation in isotropic solids. *Acta Metall., 10,* 907–913.

Cameron, M., S. Sueno, C. T. Prewitt and J. J. Papike (1973) High-temperature crystal chemistry of acmite, diopside, hedenbergite, jadeite, spodumene, and ureyite. *Am. Mineral., 58,* 594–618.

Ferry, J. M. and J. G. Blencoe (1978) Subsolidus phase relations in the nepheline–kalsilite system at 0.5, 2.0, and 5.0 kbar. *Am. Mineral., 63,* 1225–1240.

Fletcher, R. C. and R. H. McCallister (1974) Spinodal decomposition as a possible mechanism in the exsolution of clinopyroxene. *Carnegie Inst. Wash. Year Book, 73,* 396–399.

Grundy, H. D. and W. L. Brown (1969) A high temperature X-ray study of the equilibrium forms of albite. *Mineral. Mag., 37,* 156–172.

Haggerty, S. E. (1976) Opaque mineral oxides in terrestrial igneous rocks. In D. Rumble, Ed., *Oxide Minerals,* p. Hg101–Hg300. Mineral. Soc. Am. Short Course Notes 3.

Henderson, C. M. B. and J. Ellis (1976) Thermal expansion of synthetic alkali feldspars. *Progress in Experimental Petrology at Manchester University.* p. 55–59. Natural Environment Research Council, Publ. Series D, No. 6.

Kroll, H. and H. U. Bambauer (1971) The displacive transformation of (K,Na,Ca)-feldspars. *Neues Jahrb. Mineral. Monatsh.,* 413–416.

Kushiro, I. (1972) Determination of the liquidus relations in synthetic silicate systems with electron probe analyses. The system forsterite–diopside–silica at 1 atmosphere. *Am. Mineral., 57,* 1260–1271.

Lally, J. S., A. H. Heuer and G. L. Nord, Jr. (1974) Transmission microscopy study of precipitation in hematite–ilmenite (abstr.). *Geol. Soc. Am. Abstracts with Programs, 6,* 835.

Lindsley, D. H. (1965) Iron–titanium oxides. *Carnegie Inst. Wash. Year Book, 64,* 144–148.

——— (1973) Delimitation of the hematite–ilmenite miscibility gap. *Geol. Soc. Am. Bull., 84,* 657–661.

McCallister, R. H. and R. A. Yund (1977) Coherent exsolution in Fe-free pyroxenes. *Am. Mineral., 62,* 721–726.

Newton, R. C., T. V. Charlu, P. A. M. Anderson and O. J. Kleppa (1979) Thermochemistry of synthetic clinopyroxenes on the join $CaMgSi_2O_6$–$Mg_2Si_2O_6$. *Geochim. Cosmochim. Acta, 43,* 55–60.

Nye, J. F. (1957) *Physical Properties of Crystals.* Oxford University Press, London.

Orville, P. M. (1967) Unit-cell parameters of the microcline–low albite and the sanidine–high albite solid solution series. *Am. Mineral., 52,* 55–86.

Parsons, I. (1978) Alkali-feldspars: which solvus? *Phys. Chem. Minerals, 2,* 199–214.

Robin, P.-Y. F. (1974a) Thermodynamic equilibrium across a coherent interface in a stressed crystal. *Am. Mineral., 59,* 1286–1298.

——— (1974b) Stress and strain in cryptoperthite lamellae and the coherent solvus of alkali feldspars. *Am. Mineral., 59,* 1299–1318.

——— (1977) Angular relationships between host and lamellae and the use of the Mohr circle. *Am. Mineral., 62,* 127–131.

Robinson, P., M. Ross, G. L. Nord, Jr., J. R. Smyth and H. W. Jaffe (1977) Exsolution lamellae in augite and pigeonite: fossil indicators of lattice parameters at high temperature and pressure. *Am. Mineral., 62,* 857–873.

Rumble, D., III (1976) Oxide minerals in the metamorphic rocks. In D. Rumble, Ed., *Oxide Minerals,* p. R1–R24. Mineral. Soc. Am. Short Course Notes 3.

Ryzhova, T. V. and K. S. Aleksandrov (1962) Elastic properties of rock-forming minerals. IV. Nephelite. *Bull. (Izv.) Acad. Sci. USSR, Geophys. Ser.,* 1799–1801. [trans. *Am. Geophys. Union,* 1125–1127 (1962)].

Sahama, T. G. (1960) Kalsilite in the lavas of Mt. Nyirangongo (Belgian Congo). *J. Petrol., 1,* 146–171.

Sipling, P. J. and R. A. Yund (1976) Experimental determination of the coherent solvus for sanidine–high albite. *Am. Mineral., 61,* 897–906.

Smith, J. V. (1969a) Crystal structure and stability of the $MgSiO_3$ polymorphs; physical properties and phase relations of Mg,Fe pyroxenes. *Mineral Soc. Am. Spec. Pap., 2,* 3–29.

——— (1969b) Magnesium pyroxene at high temperature: inversion in clinoenstatite. *Nature, 222,* 256–257.

Smith, P. and I. Parsons (1974) The alkali-feldspar solvus at 1 kilobar water-vapor pressure. *Mineral. Mag., 29,* 747–767.

Thompson, J. B., Jr. (1967) Thermodynamic properties of simple solutions. In P. H. Abelson, Ed., *Researches in Geochemistry II,* p. 340–361. Wiley, New York.

——— and D. R. Waldbaum (1969) Mixing properties of sanidine crystalline solutions: III. Calculations based on two-phase data. *Am. Mineral., 54,* 811–838.

Tullis, J. (1975) Elastic strain effects in coherent perthitic feldspars. *Contrib. Mineral. Petrol., 49,* 83–91.

Turnock, A. C., D. H. Lindsley and J. E. Grover (1973) Synthesis and unit cell parameters of Ca–Mg–Fe pyroxenes. *Am. Mineral., 58,* 50–59.

Voight, W. (1907) Bestimmung der Elastizitatskonstanten von Eisenglanz. *Ann. Phys., 22,* 129–140.

Willaime, C. and W. L. Brown (1974) A coherent elastic model for the determination of the orientation of exsolution boundaries: application to the feldspars. *Acta Crystallogr., A30,* 316–331.

Yund, R. A. (1974) Coherent exsolution in the alkali feldspars. In A. W. Hofmann, B. J. Giletti, H. S. Yoder and R. A. Yund, Eds., *Geochemical Transport and Kinetics,* p. 173–184. Academic Press, New York.

———, R. H. McCallister and S. M. Savin (1972) An experimental study of nepheline–kalsilite exsolution. *J. Petrol., 13,* 255–272.

Manuscript received, October 25, 1978;
accepted for publication, April 23, 1979.